

**Magnetization reversal in an Fe film with an array of elliptical holes on a square lattice**

I. Guedes\* and M. Grimsditch

*Materials Science Division, Argonne National Laboratory, Argonne, Illinois 60439*

V. Metlushko

*Department of Electrical and Computer Engineering, University of Illinois at Chicago, Chicago, Illinois 60607*

P. Vavassori

*INFN UdR of Ferrara–Dipartimento di Fisica, Università di Ferrara and INFN–National Research Center on nanoStructures and bioSytsems at Surfaces, I-44100 Ferrara, Italy*R. Camley<sup>†</sup>*Physics Department, University of Colorado, Colorado Springs, Colorado 80933*

B. Ilic

*School of Applied and Engineering Physics, Cornell University, Ithaca, New York 14853*

P. Neuzil and R. Kumar

*Institute of Microelectronics, 11 Science Park Road, 117685, Singapore*

(Received 25 June 2002; revised manuscript received 6 September 2002; published 30 January 2003)

The reversal mechanism for the magnetization in an Fe film with an array of elliptical holes is investigated using the diffracted magneto-optic Kerr effect (D-MOKE) technique. D-MOKE results are obtained as a function of temperature and the angle between the applied magnetic field and an ellipse axis. The transverse and longitudinal magnetization components and minor magnetization loops are also explored in order to understand the reversal process. The experimental results are interpreted using micromagnetic simulations. The simulations account for the strong angular dependence of the hysteresis loops and provide a detailed picture of how the local magnetization evolves during reversal. The actual reversal process occurs neither by coherent rotation of domains nor by clear domain-wall motion: domain smearing appears to be a more suitable description of the phenomenon.

DOI: 10.1103/PhysRevB.67.024428

PACS number(s): 75.60.Jk, 78.20.Ls, 75.30.Gw

**INTRODUCTION**

Arrays of micron- and submicron-sized holes in a continuous ferromagnetic film have been proposed as a competitor for high-density storage media, with characteristics of high stability while avoiding the superparamagnetic limit.<sup>1</sup> The introduction of arrays of holes in magnetic thin films also provides a means of engineering their magnetic properties in a controllable way.<sup>1,2</sup> The switching mechanism during magnetization reversal is an important issue, which is not yet well understood in these systems.<sup>1–6</sup> In a recent article we presented the results of a diffracted magneto-optic Kerr effect (D-MOKE) investigation of an array of elliptical holes in an Fe film.<sup>7</sup> There we showed how the D-MOKE signal is related, through the magnetic form factor, to the domain structure that exists during reversal. We also showed that when the field is applied along the long axis of the ellipses only a small fraction of the sample develops domains while extensive “stripe” domains, that connect next-nearest ellipses, form when the field is applied along the ellipse’s short axis. In that investigation no attempt was made to extract from the D-MOKE results how the domains formed and/or transformed during reversal.

The sample investigated here is the same one investigated in Ref. 7, viz., an Fe film with nanometric elliptical holes

forming a square  $1 \times 1\text{-}\mu\text{m}^2$  lattice. Here we report a comprehensive study of the D-MOKE results as a function of the angle between the applied field and the ellipse axis, the temperature, the transverse and longitudinal magnetization, and minor magnetization loops (i.e., loops in which the maximum and minimum fields are not equal). The results are interpreted using the form factor approach described in Ref. 7. The analysis of D-MOKE loops has been improved by extracting field-dependent form factors from micromagnetic simulations. In spite of the difficulties associated with micromagnetic simulations of negative arrays (viz., dealing with the boundary conditions), such calculations enable full hysteresis loops from any interference order to be calculated, and simultaneously yield a detailed picture of how the local magnetization evolves during reversal.

**EXPERIMENTAL DETAILS AND PREVIOUS RESULTS**

Details of the sample fabrication were previously described in Ref. 7. Briefly, the sample is an Fe film, 60 nm thick, with elliptical holes  $\approx 200$  nm wide by  $\approx 800$  nm long, forming a square  $1 \times 1\text{-}\mu\text{m}^2$  lattice. A transmission scanning electron microscopy image of the sample is shown in Fig. 1(a).

MOKE experiments were performed in the “transverse Kerr” geometry. Incident,  $p$ -polarized light, on the sample was detected in the scattering plane with no analyzer. This

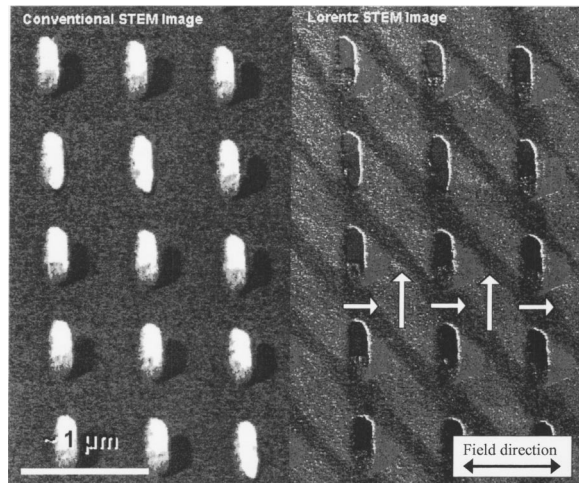


FIG. 1. (a) Scanning transmission electron microscopy (STEM) image of our array of elliptical holes in a 60-nm-thick Fe film. (b) Lorentz STEM image of the same sample; the arrows are the magnetization directions inferred from D-MOKE analysis.

configuration is sensitive only to the component of  $M$  perpendicular to the scattering plane. By applying a field ( $H$ ) perpendicular to the scattering plane we obtain the magnetization parallel to  $H$  (longitudinal magnetization component), with  $H$  in the film plane and in the scattering plane we obtain the component of  $M$  perpendicular to  $H$  (transverse magnetization component).

The basic formalism developed to interpret D-MOKE results was presented in Refs. 7 and 8. In Ref. 7 the domain structure at remanence was inferred from simple energy considerations. In Ref. 8 and here we obtain form factors as a function of field from micromagnetic simulations. Micromagnetic calculations were performed using the web version of the NIST code.<sup>9</sup> The difficulties of using this approach for negative arrays will be discussed.

Figure 1(b) is the Lorentz microscopy image showing the domain structure, deduced from the D-MOKE,<sup>7</sup> that forms when the field is applied along the short ellipse axis. The form factors of these domains provide a qualitative explanation of the salient features of the longitudinal D-MOKE loops shown in Figs. 2(d)–2(f). Because the domains that form when the field is applied along the long axis of the ellipses are quite small, their effect on the D-MOKE loops [Figs. 2(a)–2(c)] is also small. For this reason, in this paper, we will concentrate on the magnetization reversal for fields that are roughly along the ellipse's short axis.

## RESULTS

### Angular dependence of transverse and longitudinal magnetization

Figure 3 shows the zeroth- and first-order longitudinal and first-order transverse loops measured as a function of the angle ( $\phi$ ) between the applied field and the ellipse's short axis. (The zeroth-order transverse loops are noisy but mimic the first-order ones). For  $\phi = 0^\circ \pm 1.5^\circ$  we find that the loops

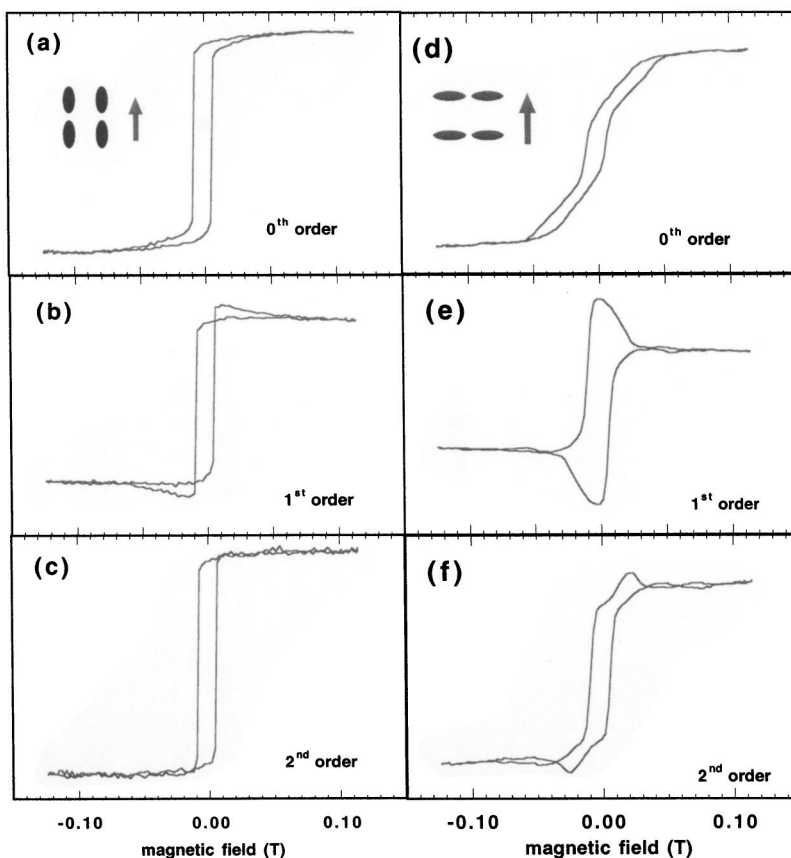


FIG. 2. Longitudinal D-MOKE loops of various orders, from the patterned area of the film. The applied field is along the long and short axes of the ellipses.

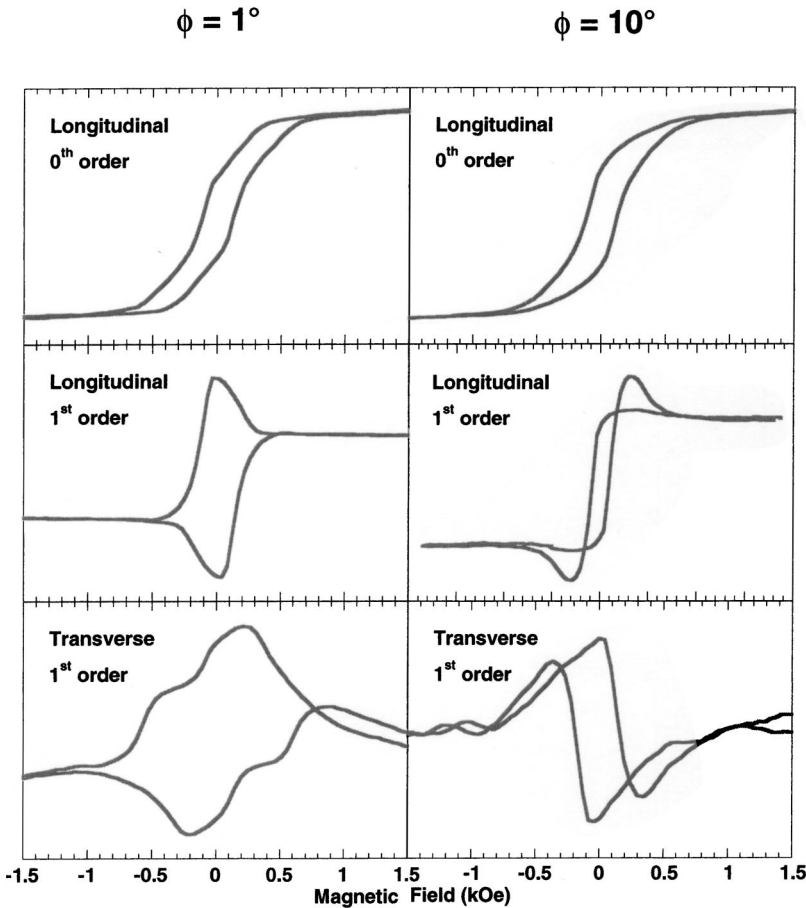


FIG. 3. Experimental D-MOKE loops vs angle ( $\phi$ ) between field and short ellipse axis: zeroth- and first-order longitudinal and first-order transverse.

have quite different shapes than for  $\phi > 2^\circ$ . As will be shown in a quantitative fashion in the next section, these differences can be traced to the manner in which “domains” are initially nucleated. Qualitatively, as discussed in Ref. 7, the increase in the first-order longitudinal D-MOKE signal at low values of  $H$  with respect to its value when the sample is saturated (high values of  $H$ ), is due to the formation of domains. The different shapes of the loops in Fig. 3 indicate that when the field is along the hard axis ( $\phi = \pm 1.5^\circ$ ), the onset of magnetization reversal is retarded, and considerably more domain formation occurs prior to reversal. As the angle  $\phi$  is varied (either increased or decreased), domains are present both before and after reversal, and the value of  $H$  at which the reversal occurs becomes lower as  $\phi$  increases.

#### Minor loops

Loops in the left column of Fig. 4 show experimental first-order longitudinal D-MOKE loops as a function of the maximum positive field applied during the hysteresis cycle. While the zeroth-order loops (not shown) show only minor changes as the maximum field of the loop is changed, the first-order loops show substantial differences close to the reversal field. In particular, the negative overshoot on the decreasing side of the loop, which is almost absent in the full loop, becomes a prominent feature for the asymmetric loops. These changes will again be traced to the way in which domains are nucleated and annihilated.

#### Temperature dependence

Figure 5 shows zeroth- and first-order longitudinal D-MOKE loops as a function of temperature ( $H$  is applied at a small angle from the short axis of the ellipses). We observe no substantial changes in the hysteresis loops as the temperature is lowered. As discussed in Ref. 7, the magnetization reversal occurs via the nucleation of demagnetizing-field-induced  $90^\circ$  domains, which form to reduce the dipolar magnetostatic energy associated with the surface charges that appear at the hole edges.<sup>10,11</sup> The minor modifications of the D-MOKE loops vs temperature provides evidence that thermal activation does not play a dominant role in the domain formation during reversal.

## DISCUSSION

#### Micromagnetic simulations and Theory of D-MOKE

We remind the reader that, as described in Ref. 7, the D-MOKE signals are proportional to the magnetic form factors ( $f$ ) defined by

$$f = \int_S m_y \exp[in\mathbf{G}\cdot\mathbf{r}] dS, \quad (1)$$

where  $m_y$  is the magnetization per unit area along the direction perpendicular to the scattering plane,  $n$  is the interference order,  $\mathbf{G}$  is the reciprocal-lattice wave vector, and the

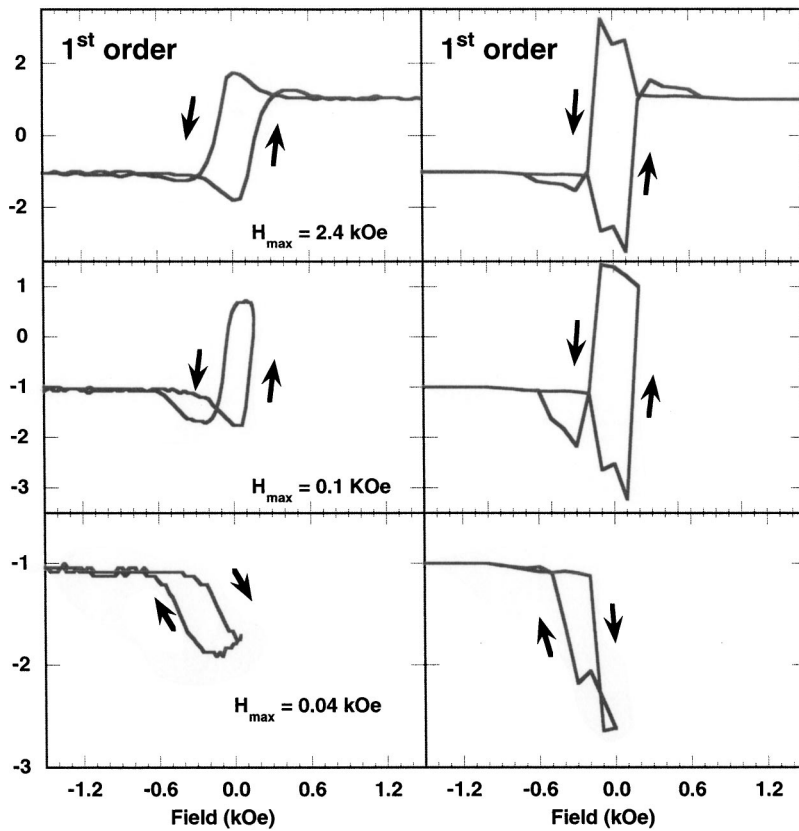


FIG. 4. Experimental (left) and simulated (right) first-order longitudinal loops as a function of maximum applied positive field.

integration is carried out over a unit cell of the array. Note that for  $n=0$  (i.e., the reflected spot) Eq. (1) is just the integral of  $M_y$ , and hence yields the same information as conventional MOKE. In Ref. 7 it was assumed that at some instant during each hysteresis loop domain formation was complete in the sense that it was the same in all unit cells. With this assumption it was shown that the domains displayed in Fig. 1(b) were consistent with the maximum increases or decreases observed in the loops. No attempt was

made in that investigation to explain how domains appear and evolve during the switching. Here we wish to examine if the path taken during domain formation can be extracted from the data presented in Figs. 2–4.

The field-dependent form factors can, in principle be extracted from micromagnetic simulations.<sup>8</sup> At each field the distribution of spins is extracted from the simulation and, using Eq. (1), the form factors obtained. Although this approach works remarkably well for a system of circular

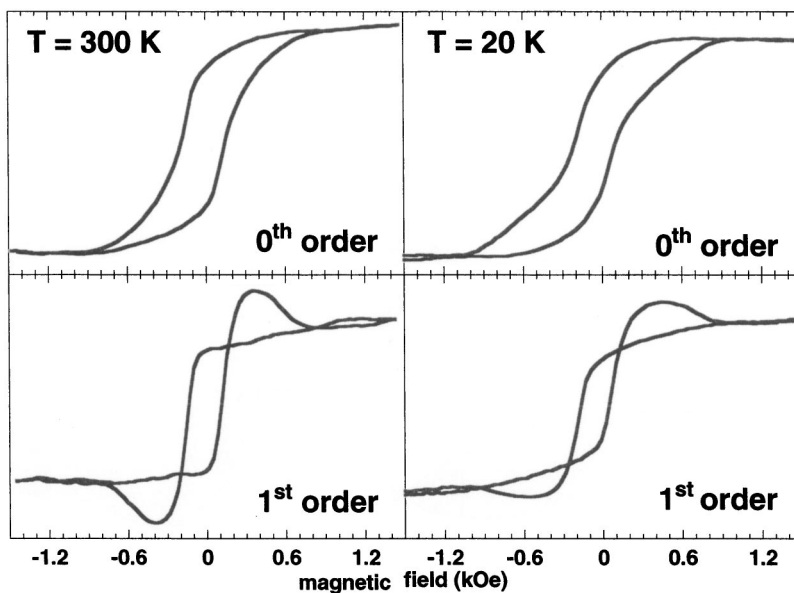


FIG. 5. Temperature dependence of zeroth- and first-order longitudinal loops.



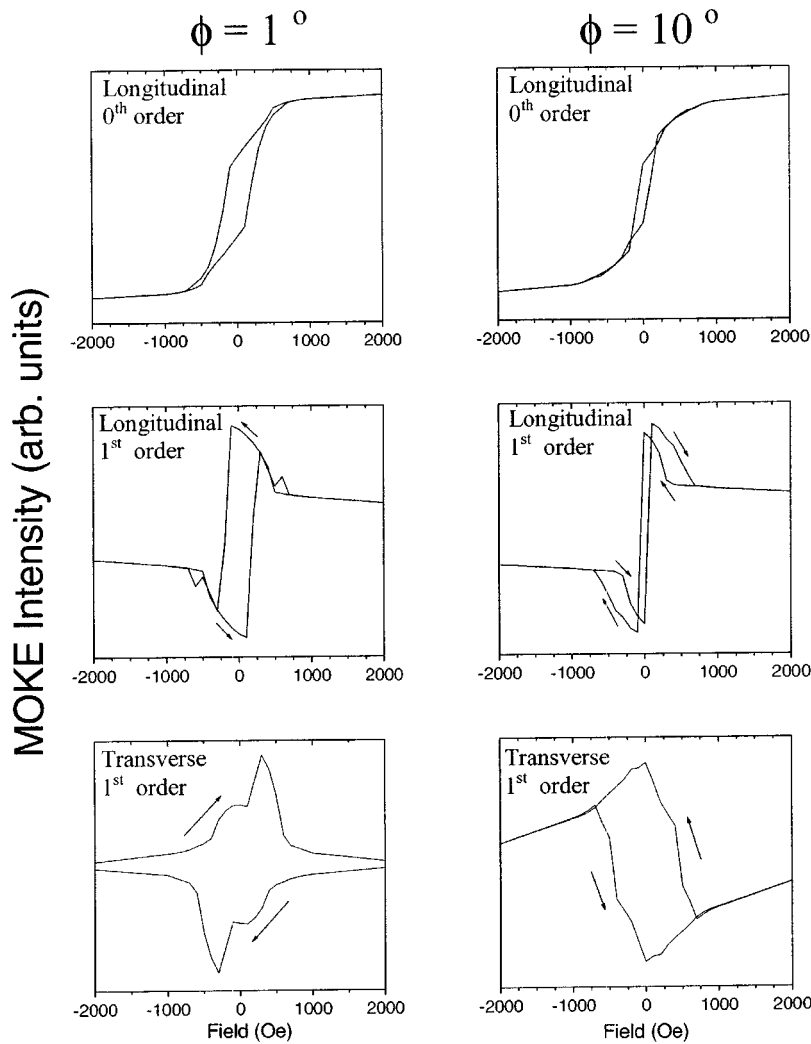


FIG. 6. Calculated loops: zeroth- and first-order longitudinal, and first-order transverse for  $\phi$  equal to  $1^\circ$  and  $10^\circ$ .

disks,<sup>12</sup> it encounters some difficulties when applied to an array of holes as in the present case. The origin of the difficulty lies in establishing appropriate boundary conditions (BCs). From a calculation standpoint it is desirable to perform the simulation on a single unit cell of the negative array. This approach requires the introduction of periodic BCs necessary to deal with an extended structure. Introducing the correct BCs for this approach to be valid is, however, far from trivial. Conceptually it would be easy to introduce the exchange coupling at the boundaries of the unit cell by coupling each edge to its opposite side. The dipolar terms, however, are not amenable to such a simple solution since they depend on the distribution of charges throughout the neighboring cells. In the absence of a suitable way of introducing the BCs, we have resorted to the brute force approach in which a large system, comprised of many unit cells, is simulated. Here again some compromises must be reached. Edge effects, that enhance magnetization rotation when  $M$  is perpendicular to an edge (i.e., favoring domain nucleation) and hinder its rotation when  $M$  is parallel to an edge (i.e., inhibiting domain nucleation or rotation), are reduced by simulating a structure with rough edges. The roughening is accomplished by alternately removing a computational cube from around the edges. Although this reduces the effect of

the outer edges on the central cells, the simulations invariably show a non uniform formation of domains in different unit cells. Ideally the size of the system could be increased until a uniform domain structure is found for the central cells. In our case, even for a  $5 \times 5$  unit cells system we were not in that regime. Larger systems required unacceptable calculation times. Our simulated structure consisted of  $5 \times 5$  unit cells each one consisting of  $21 \times 21$  calculation cells (for a total of 11 025 computational cubic cells each one with a side of 48 nm) and the outer edges were roughened. The material parameters of Fe, with the anisotropy set to zero, were used for the simulations. The form factors were calculated for the central unit cell of the  $5 \times 5$  simulation.

#### Comparison between measurements and theory

Figure 6 shows the zeroth- and first-order longitudinal loops and first-order transverse loops, calculated from the form factors. The applied field was at  $1^\circ$  and  $10^\circ$  from the ellipse's short axis. The loops in Fig. 6 qualitatively reproduce the experimental hysteresis loops in Fig. 3. Both experimental and simulated loops show that the zero-order loops are not greatly affected by the changes in field direction. For

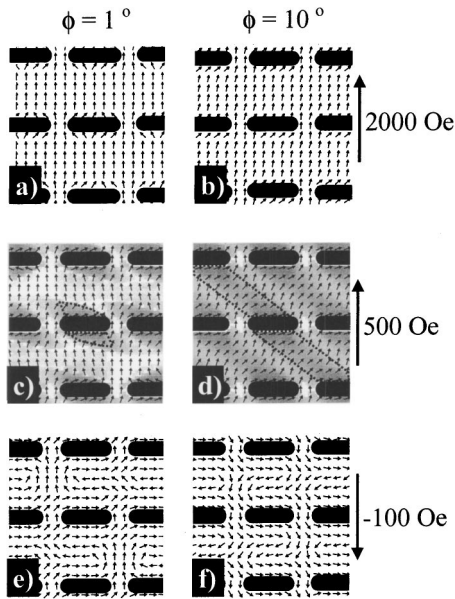


FIG. 7. Micromagnetic domains vs  $H$  (2000, 500, and  $-100$  Oe) and angle  $\phi$  ( $1^\circ$  and  $10^\circ$ ). In panels (c) and (d) a gray-scale proportional to the magnetization component perpendicular to the short axis of the ellipses is used to highlight the domain structure. The dotted lines are a guide to the eye.

the first-order longitudinal and transverse loops the shape changes can be ascribed to variations in the domain structure during reversal.

In Fig. 7 we show the micromagnetic spin configurations at various fields for the two directions of the applied field. Figure 7(d) shows the previously reported<sup>7</sup> stripelike domains, with the magnetization vector at  $\approx 90^\circ$  with respect to the initial saturation direction. These domains bridge next-nearest-neighboring holes along the lattice diagonal, when  $H$  is applied at  $10^\circ$ . For  $H$  applied almost along the short ellipse axis, Fig. 7(c) shows that domain nucleation is hindered and, when it does occur, is different from that for the  $10^\circ$  angle. Indeed, the comparison of Figs. 7(c) and 7(d) shows that for  $H = 500$  Oe the  $90^\circ$  domains are less extended in the case of  $H$  applied almost along the short ellipse axis, and they form short blades that do not overlap with those from next-nearest neighboring holes. Figures 7(e) and 7(f) show that when  $H$  is reversed ( $H = -100$  Oe) an intricate domain structure is generated. A detailed comparison of these two figures shows that the average magnetization component parallel to  $H$  has changed sign (i.e., the jump in the hysteresis loops has already occurred) only when  $H$  is applied at  $10^\circ$ . This is in agreement with the retarded magnetization reversal observed experimentally when  $H$  is close to the hard axis. Also evident in Fig. 7 is that reversal does not occur via an obvious domain wall motion nor by coherent rotation. It is perhaps more suitable to describe the reversal process as domain smearing.

The experimental full loop in Fig. 4 is indicative that if the sample approaches reversal after being saturated, most of the ‘domain’ formation occurs *before* reversal (viz., the peaks in the first-order loops are larger before than after reversal). As the maximum field is reduced, the intensity of the two

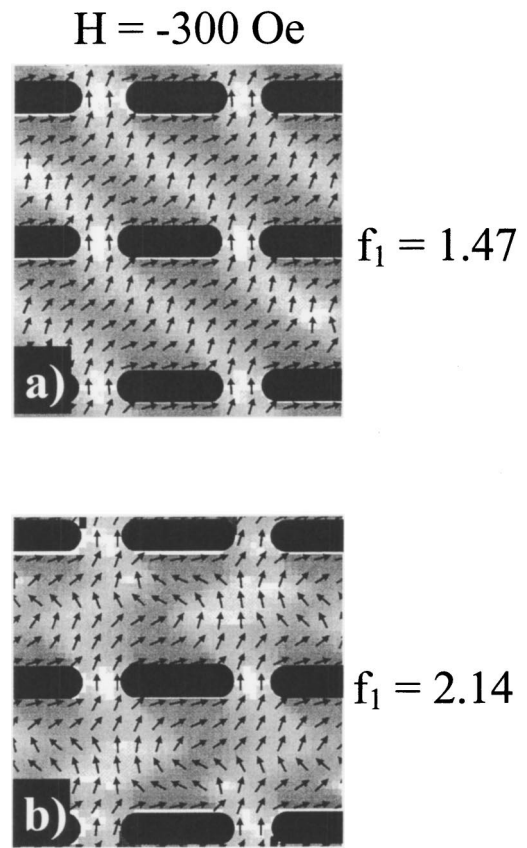


FIG. 8. Domains in minor loops at the same field ( $-300$  Oe) but for different max fields: panel (a) maximum field  $2500$  Oe, panel (b) maximum field  $300$  Oe.

peaks, *after* and *before* reversal, become comparable (middle loop). Loops in the right column of Fig. 4 show the first-order longitudinal loops calculated using the form factor  $f_1$  extracted from micromagnetic simulations as a function of the maximum positive field applied during the hysteresis cycle. The qualitative agreement with the measured D-MOKE loops is remarkable. In Fig. 8 we show two spin distributions at the same field  $H = -0.3$  kOe but reached from different maximum fields:  $2.5$  [Fig. 8(a)] and  $0.3$  kOe [Fig. 8(b)], corresponding to the loops shown in Figs. 4(a) and 4(c) respectively. Also indicated in Fig. 8 are the first-order form factors for the two states, normalized to the value of  $f_1$  at saturation (we actually used the value of  $f_1$  at  $H = 2.5$  kOe.) The increase of  $f_1$  for the state reached from a lower maximum field [Fig. 8(b)] reflects the larger deviation from the saturated state and provides the explanation for the loops in Fig. 4.

## CONCLUSIONS

We have used the D-MOKE technique to investigate the reversal mechanism in an array of elliptical holes in an Fe film. Experimentally, based on the changes in the various diffracted hysteresis loops, we find that the reversal process depends quite strongly on the angle between the magnetic field and the ellipse axis. In spite of boundary condition difficulties, we have used micromagnetic simulations to inter-

pret the experimental results. The micromagnetic boundary condition problems were partially circumvented by introducing rough edges on the simulated sample and by using the largest sample consistent with acceptable computing times. The simulations account for the strong angular dependence of the hysteresis loops. They also show the angular dependence of the domain structure generated during reversal. The actual reversal process occurs neither by a coherent rotation of domains nor by clear domain wall motion: domain smearing appears to be a more suitable description of the phenomenon.

### ACKNOWLEDGMENTS

Work at ANL was supported by the U.S. Department of Energy, BES, Materials Science under Contract No. W-31-109-ENG-38, and at the University of Illinois by NSF Grant No. ECS-0202780. P.V. acknowledges financial support from MURST-COFIN 2000 and INFN “MAGDOT” PAIS research programs. I.G. acknowledges financial support from CNPq Brazilian Funding Agency. R.C. was supported by US Army Research Office under DAAD19-02-1-0174. Our thanks to Dr. N. Zaluzec for permission to reproduce his STEM image from Ref. 7.

\*Present address: Departamento de Física, UFC Caixa Postal 6030, Campus do Pici 60455-760 Fortaleza CE, Brazil.

<sup>†</sup>Visiting scientist at MSD, ANL during the summer of 2001.

<sup>1</sup>R. P. Cowburn, A. O. Adeyeye, and J. A. Bland, *Appl. Phys. Lett.* **70**, 2309 (1997); *J. Magn. Magn. Mater.* **173**, 193 (1997).

<sup>2</sup>L. Torres, L. Lopez-Diaz, and J. Iñiguez, *Appl. Phys. Lett.* **73**, 3766 (1998).

<sup>3</sup>C. A. Grimes, P. L. Trouilloud, J. K. Lumpp, and G. C. Bush, *J. Appl. Phys.* **81**, 4720 (1997).

<sup>4</sup>Y. Otani, S. G. Kim, T. Kohda, K. Fukamichi, O. Kitakami, and Y. Shimada, *IEEE Trans. Magn.* **34**, 1090 (1998).

<sup>5</sup>L. Torres, L. Lopez-Diaz, O. Alejos, and J. Iñiguez, *J. Appl. Phys.* **85**, 6208 (1999).

<sup>6</sup>C. T. Yu, H. Jiang, L. Shen, P. J. Flanders, and G. J. Mankey, *J. Appl. Phys.* **87**, 6322 (2000).

<sup>7</sup>I. Guedes, N. J. Zaluzec, M. Grimsditch, V. Metlushko, P. Vavassori, B. Ilic, P. Neuzil, and R. Kumar, *Phys. Rev. B* **62**, 11 719

(2000).

<sup>8</sup>I. Guedes, M. Grimsditch, V. Metlushko, P. Vavassori, R. Camley, B. Ilic, P. Neuzil, and R. Kumar, *Phys. Rev. B* **66**, 014434 (2002).

<sup>9</sup>OOMMF User's Guide, Version 1.0., M. J. Donahue and D. G. Porter. Interagency Report NISTIR 6376. National Institute of Standards and Technology, Gaithersburg, MD (Sep 1999). (<http://math.nist.gov/oommf/>)

<sup>10</sup>P. Vavassori, V. Metlushko, R. M. Osgood, M. Grimsditch, U. Welp, G. Crabtree, W. Fan, S. Brueck, B. Ilic, and P. Hesketh, *Phys. Rev. B* **59**, 6337 (1999).

<sup>11</sup>S. Chiczumi and S. Charap, *Physics of Magnetism* (Wiley, New York, 1964).

<sup>12</sup>M. Grimsditch, P. Vavassori, V. Novosad, V. Metlushko, H. Shima, Y. Otani, and K. Fukamichi, *Phys. Rev. B* **65**, 172419 (2002).